ELSEVIER

Physica C 293 (1997) 77–81

PHYSICA C

Superconductive tunneling in junctions with resonant double barrier structures

G. Johansson [a,*], V.S. Shumeiko [a,b], E.N. Bratus' [a,b], G. Wendin [a]

[a] *Department of Microelectronics and Nanoscience, Chalmers University of Technology, S-412 96 Göteborg, Sweden*
[b] *B. Verkin Institute for Low Temperature Physics and Engineering, 310164 Kharkov, Ukraine*

Abstract

We calculate the current–voltage characteristics (IVC) of a biased superconducting junction with a tunnel resonance. Within a simple one-dimensional model we discuss how the IVCs depend on the position and width of the resonance. We consider both subgap region and excess current. The results provide a possible explanation of the anomaly in the onset of c-axis current in recent experiments on intrinsic Josephson effect in BSCCO. © 1997 Elsevier Science B.V.

1. Introduction

Interpretation of experimental results on intrinsic Josephson effect in layered high-T_c superconductors [1–4] presents a challenge for theory, even if restricted to a simple BCS model, because of the possibility of resonant tunneling. An elementary c-axis cell, e.g. of Bi2212, contains a Bi–O double layer separated from the superconducting Cu–O planes by tunnel barriers formed by Sr–O layers. This double barrier structure may cause resonant tunneling between the Cu–O planes.

Meanwhile, a theory of resonant tunneling in *biased* superconducting junctions is poorly developed. In particular, nothing is known about the subharmonic gap structure in resonant tunnel junctions or about the dependence on position and width of the resonance. Such information should be obtained from the analysis of multiparticle tunneling in resonant junctions. In this communication we present some results on this subject.

2. The model

The Intrinsic Josephson Effect (IJE) in layered cuprates consists of the development of a resistive current state, with (in the simplest case) supercurrent flow interrupted within a single cell between two neighbouring Cu–O planes. A finite voltage drop appears at this cell, while the rest of the sample remains in the superconducting state and carries the supercurrent. We model this structure in the form of two bulk BCS-like superconductors (Cu–O planes) connected by a non-superconducting region which consists of a normal quantum well (Bi–O layers) separated from the superconducting electrodes by tunnel barriers of similar shape (Sr–O layers). We assume the structure to be homogeneous in the plane

* Corresponding author. Tel.: +46 31 772 8032; fax: +46 31 772 3436; e-mail: tfygj@fy.chalmers.se.

0921-4534/97/$17.00 © 1997 Elsevier Science B.V. All rights reserved.
PII S0921-4534(97)01518-9

of the junction, which makes the tunneling problem essentially one-dimensional.

In the mesoscopic scenario of superconductive tunneling [5,6], the tunnel current is associated with quasiparticle scattering states originating from superconducting electrodes. Such states consist of many inelastic channels due to multiple Andreev reflections occurring in biased superconducting junctions. Based on such an approach, calculation of current–voltage characteristics (IVC) of nonresonant tunnel junctions has previously been performed. In this paper we will generalize our method to the resonant case.

We will assume that the tunneling amplitude consists of a single Breit–Wigner resonance near the Fermi level,

$$t(E) = \frac{\Gamma}{(E - E_0) + i\Gamma}, \qquad (1)$$

where E_0 is the position of the resonance and Γ is the resonance half-width, energy being counted from the Fermi level. We will consider the most interesting, and at the same time most complex, case when both the position and the width of the resonance are comparable to, or smaller than, the superconducting energy gap: E_0, $\Gamma \sim \Delta$. Using a general approach developed in [7], it is possible to formulate the boundary condition for the Bogoliubov–de Gennes equation, describing tunnel junctions, in terms of a transfer matrix related to the normal transition amplitude in Eq. (1). Recurrence relations for the multiple Andreev reflection amplitudes can then be derived, which allows a complete calculation of the IVC of the resonant junction.

3. Results

We have numerically calculated the current–voltage characteristics at zero temperature $T = 0$ for different E_0 and Γ. The current is measured in units of the current through the resonance in the normal state I_N for large bias $eV \gg E_0$, where $I_N \sim \Gamma$. We take into account the displacement of the resonance due to the applied voltage, considering two limiting cases for this dependence. First, we consider a 'symmetric' junction where E_0 is independent of bias, and then an 'asymmetric' junction where the resonance follows one of the chemical potentials.

3.1. Symmetric junction

In symmetric junctions E_0 is counted from the midpoint between the shifted chemical potentials of the electrodes. Fig. 1 shows an IVC for a symmetric junction with $E_0 = 0$. Worth noting is the negative differential conductivity above the onset of the current in the region below $eV = \Delta$, as well as the strong suppression the subgap structure at $eV = \Delta$. The logplot of the subgap region (inset) shows that this suppression is a general phenomenon, i.e. no structures are visible at bias voltages $eV = 2\Delta/n$ when n is even. There is also negative differential conductance just above the onset of every odd subgap structure.

The details of the IVC in Fig. 1 can be understood from the interplay of resonance and multiparticle tunneling processes: either process undergoes resonant enhancement depending on bias voltage and position of the resonance. Fig. 2 shows the three lowest order resonant processes. The main current step is described by process A. This is a single particle process involving no Andreev reflections and it dominates at $eV > 2\Delta$.

The suppression of the first subgap structure at $eV = \Delta$ can be explained in the following way: In

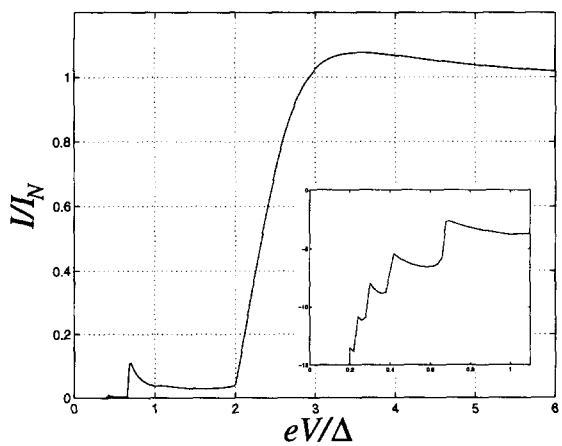

Fig. 1. IVC for a symmetric junction. Resonance position $E_0 = 0$ (midpoint between the left-right chemical potentials) and width $\Gamma = 0.2\Delta$.

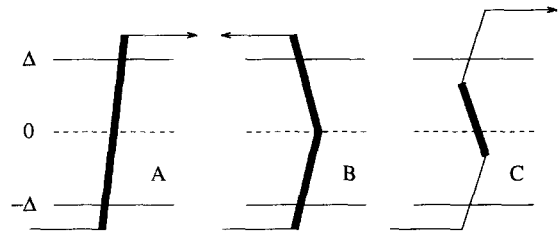

Fig. 2. Diagrams of the three lowest-order resonant processes. Bold lines denote resonant transitions. Processes A, B, C involve 0, 1, and 2 Andreev reflections, respectively.

non-resonant junctions, process B – which involves one Andreev reflection – dominates at $eV > \Delta$, while process C – which involves two Andreev reflections – dominates below $eV = \Delta$.

In our case, with a resonant level positioned at the average chemical potential ($E_0 = 0$), process B remains non-resonant (described by a modified Fig. 2(b) with only thin lines) while process C is enhanced by the resonance and dominates both below and above $eV = \Delta$. In the same manner every process with even number of Andreev reflections is enhanced by the resonance and dominates over the processes with odd number of reflections. This leads to apparent suppression of the even subgap structures.

The negative differential conductance seen above the odd subgap thresholds is a result of the increased density of states near the gap – the dominant process is enhanced by this increased density of states, which results in a peak in the IVC.

Fig. 3 shows the dependence of the IVC on the position of the resonance E_0. In these curves the onset of the main current is more gradual than in Fig. 1. This is because the bias at which process A becomes fully resonant grows with E_0. The figure also shows tremendous enhancement of the structure in the region $\Delta < eV < 2\Delta$ for $E_0 > 0.5\Delta$.

This enhancement of the pair current occurs because in process B both the electron and the Andreev-reflected hole can pass the junction in resonance. The pair current peak moves to higher voltage with growing E_0. This effect has a similar explanation as the shift of the main-current onset: the bias at which process B becomes fully resonant grows with E_0.

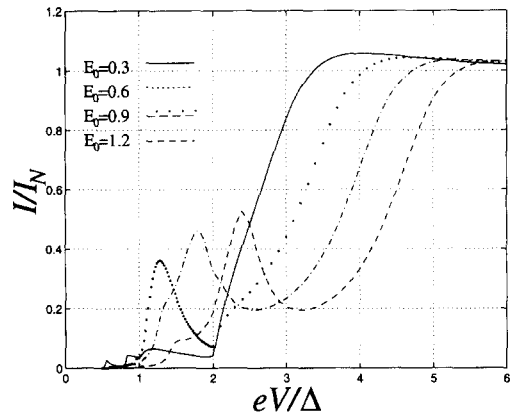

Fig. 3. IVC for a symmetric junction for different positions E_0 of the resonant level. $E_0 \in \{0.3\Delta, 0.6\Delta, 0.9\Delta, 1.2\Delta\}$ and $\Gamma = 0.2\Delta$.

In the limiting case of large $E_0 \gg \Delta$ the transparency of the junction near the gap is small and almost constant, and the IVC approaches that of a non-resonant tunnel junction.

3.2. Asymmetric junction

In the asymmetric junction, E_0 is counted from one of the chemical potentials. Fig. 4 shows the IVC of the asymmetric junction with $E_0 = 0$ (i.e. resonance at the Fermi level). The most prominent feature is the onset of the main current at $eV = \Delta$, instead of 2Δ as is the case in non-resonant junctions. This is because process B is fully resonant for

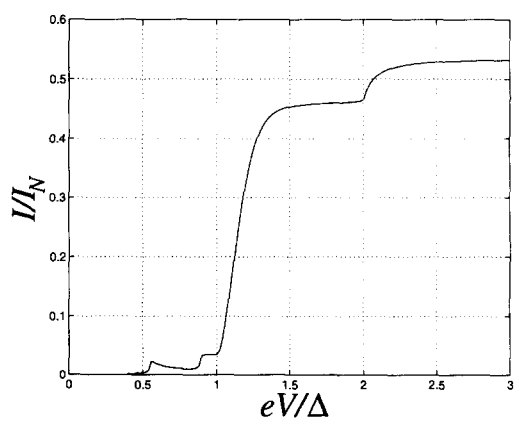

Fig. 4. IVC for an asymmetric junction. Resonance position $E_0 = 0$ (at the Fermi level) and $\Gamma = 0.2\Delta$.

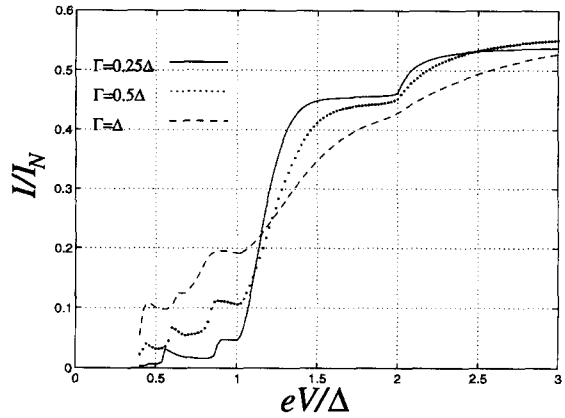

Fig. 5. IVC of asymmetric junctions with $E_0 = 0$ and $\Gamma \in \{0.25\Delta, 0.5\Delta, \Delta\}$.

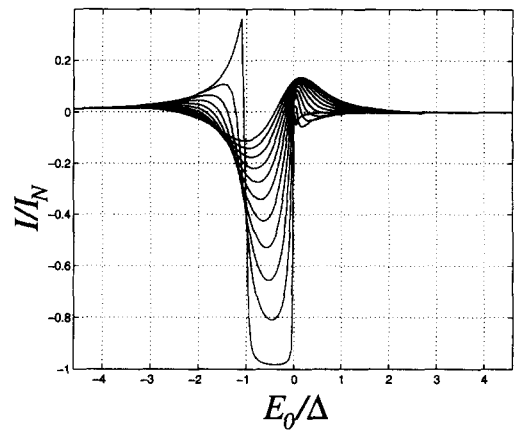

Fig. 7. Excess current versus position of resonance E_0. $\Gamma \in \{0.01\Delta, 0.11\Delta, \ldots, 1.01\Delta\}$.

$eV > \Delta$, while the normal process A never gets fully resonant and only contributes with a small step at $eV = 2\Delta$. In this case the main current is *a pair current* for all bias values.

The subgap structure at $eV = 2\Delta/3$ in Fig. 4 is strongly suppressed. This is the first sign of a suppression of every odd subgap structure, which is explained by the enhancement of processes with odd number of Andreev reflections.

Fig. 5 shows the dependence of the IVC on the resonance width Γ. For larger Γ the subgap structure grows in magnitude and loses its sharp features. Eventually, for $\Gamma \gg \Delta$, the IVC approaches SNS-like behaviour.

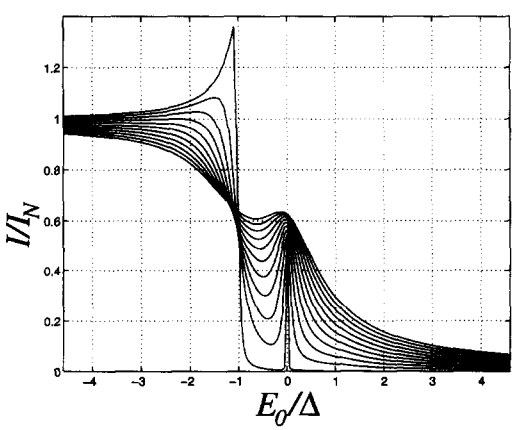

Fig. 6. Large voltage limit ($eV \gg \Delta$) of current versus position of resonance E_0. $\Gamma \in \{0.01\Delta, 0.11\Delta, \ldots, 1.01\Delta\}$.

3.3. Excess current

The dependence of the large-bias-voltage current on the position E_0 and width Γ of the resonance is shown in Fig. 6 for an asymmetric junction. To the left (E_0 below the gap), the current approaches its normal resonant value which is proportional to Γ. For a sharp resonance the effect of the superconducting density of states is clearly seen as a peak when the resonance is close to the gap-edge. There is also a peak for resonance at the chemical potential. This is an effect of process B, and for a sharp resonance the height of this peak is exactly half of the normal current to the left. To the right (E_0 above the gap), the current approaches the non-resonant value which is proportional to Γ^2. Fig. 7 shows the same as Fig. 6 but with the current in the normal state subtracted, i.e. showing the excess current. In our calculations the excess-limit is reached already for $eV > \max\{5\Delta, 2|E_0|\}$.

4. Conclusion

In plane junctions, the current results from integration over all one-dimensional scattering states with different projections of the electron momentum parallel to the plane of the junction. This involves all possible positions of the resonance, and therefore the

IVC of the plane junction will combine all features of IVCs discussed above. In particular, it will contain considerable effects of the onset of the pair current at $eV = \Delta$. This feature may explain the position of the onset of tunnel current experimentally observed in Bi2212 [1–4].

Acknowledgements

This work has been supported by grants from the Swedish agencies NFR, TFR and NUTEK, from the Royal Swedish Academy of Sciences (KVA) (E.N.B), and from the European Commission (G.W.). The hospitality of NTT Basic Research Laboratories during a sabbatical stay (GW) is gratefully acknowledged.

References

[1] R. Kleiner et al., Phys. Rev. Lett. 68 (1992) 2394.
[2] R. Kleiner, P. Müller, Phys. Rev. B 49 (1994) 1327.
[3] K. Tanabe et al., Phys. Rev. B 53 (1996) 9348.
[4] A. Yurgens et al., Phys. Rev. B 53 (1996) R8887.
[5] E.N. Bratus', V.S. Shumeiko, G. Wendin, Phys. Rev. Lett. 74 (1995) 2110.
[6] E.N. Bratus', V.S. Shumeiko, G. Wendin, Low Temp. Phys. 23 (1997) N3, Preprint cond.mat./9610101.
[7] G. Wendin, V.S. Shumeiko, Superlatt. Microstruc. 20 (1996) 569.